Fungal Genetics and Biology 122 (2019) 1–10

Contents lists available at ScienceDirect

Fungal Genetics and Biology

journal homepage: www.elsevier.com/locate/yfgbi

The acetate uptake transporter family motif "NPAPLGL(M/S)" is essential for substrate uptake

David Ribas[a], Isabel Soares-Silva[a], Daniel Vieira[a], Maria Sousa-Silva[a], Joana Sá-Pessoa[a], João Azevedo-Silva[a], Sandra Cristina Viegas[b], Cecília Maria Arraiano[b], George Diallinas[c], Sandra Paiva[a], Pedro Soares[a], Margarida Casal[a,*]

[a] Centre of Molecular and Environmental Biology (CBMA), Department of Biology, University of Minho, Campus de Gualtar, Braga 4710-057, Portugal
[b] Instituto de Tecnologia Química e Biológica António Xavier, Universidade Nova de Lisboa, Av. Da República, 2780-157 Oeiras, Portugal
[c] Department of Biology, National and Kapodistrian University of Athens, Panepistimioupolis 15781, Athens, Greece

ARTICLE INFO

Keywords:
AceTr family phylogeny
Acetate transport
Succinate transport
Carboxylate transporters
Cell membrane

ABSTRACT

Organic acids are recognized as one of the most prevalent compounds in ecosystems, thus the transport and assimilation of these molecules represent an adaptive advantage for organisms. The AceTr family members are associated with the active transport of organic acids, namely acetate and succinate. The phylogenetic analysis shows this family is dispersed in the tree of life. However, in eukaryotes, it is almost limited to microbes, though reaching a prevalence close to 100% in fungi, with an essential role in spore development. Aiming at deepening the knowledge in this family, we studied the acetate permease AceP from *Methanosarcina acetivorans*, as the first functionally characterized archaeal member of this family. Furthermore, we demonstrate that the yeast Gpr1 from *Yarrowia lipolytica* is an acetate permease, whereas the Ady2 closest homologue in *Saccharomyces cerevisiae*, Fun34, has no role in acetate uptake. In this work, we describe the functional role of the AceTr conserved motif NPAPLGL(M/S). We further unveiled the role of the amino acid residues R122 and Q125 of SatP as essential for protein activity.

1. Introduction

Organic acids are one of the most prevalent and abundant organic compounds on earth's surface and they are vital intermediates for cell metabolism (Xiao and Wu, 2014). The cell homeostasis of organisms is highly dependent on the transport of specific molecules across the cell membrane. When the environmental pH is below the p*Ka* of the acid, the protonated form predominates and crosses the cell membrane by passive diffusion according to its diffusion coefficient. However, when the pH is above the acid p*Ka* the anionic form of the acid predominates, requiring a transporter protein to cross the membrane (Casal et al., 2008; Casal et al., 2016).

The AceTr family was recently reassigned as the Acetate Uptake Transporter Family (TCDB 2.A.96) due to the functional characterization of several members as acetate transporters. AceTr proteins display six transmembrane segments (TMS), sharing the conserved motif NPAPLGL(M/F) located at the beginning of the first TMS (Augstein et al., 2003; Casal et al., 2016). Members of this family have been reported in the literature, however their function as acetate transporters has not been proven yet, namely Gpr1, Fun34 and AceP. The *Yarrowia lipolytica* Gpr1 protein, the first family member to be reported in literature, was found to be expressed in the presence of acetic acid or ethanol (Augstein et al., 2003) and it was shown to be involved in acetic acid sensitivity, cell and colony morphology, yeast-to-hyphae transition and cell lifespan (Augstein et al., 2003; Tzschoppe et al., 1999). On the other hand Ady2, the Gpr1 homologue in *Saccharomyces cerevisiae*, was found to be expressed in acetic acid grown cells, behaving as a proton-symporter for the anionic form of the acid (Casal et al., 1996; Paiva et al., 2004). The Ady2 homozygous null mutant in diploid cells results in reduced sporulation and higher frequency of abnormal asci, forming dyads instead of tetrads (Rabitsch et al., 2001). *Saccharomyces cerevisiae* has two other AceTr members, Fun34 (Ato2) and Ato3, which were reported to be involved in ammonium export, along with Ady2 (Palková et al., 2002). In the filamentous fungi *Aspergillus nidulans,* four AceTr homologs were found, AcpA, AcpB, AcpC, and AlcS, (Fillinger and Felenbok, 1996; Robellet et al., 2008; Sá-Pessoa et al., 2015). The AcpA protein is essential for the uptake and use of acetate as a sole carbon source and contributes for spore maintenance and homeostasis

* Corresponding author.
E-mail address: mcasal@bio.uminho.pt (M. Casal).

https://doi.org/10.1016/j.fgb.2018.10.001
Received 11 July 2018; Received in revised form 27 September 2018; Accepted 10 October 2018
Available online 16 October 2018
1087-1845/

(Robellet et al., 2008; Sá-Pessoa et al., 2015). AcpB was found to be responsible for residual acetate transport in mycelia, whereas no function related to carboxylic acids transport was assigned for both AcpC (Sá-Pessoa et al., 2015) and AlcS proteins (Fillinger and Felenbok, 1996; Flipphi et al., 2006). SatP is the sole AceTr homolog in *Escherichia coli*. Unlike other AceTr members, it transports both mono- and di-carboxylic acids being a succinate/acetate proton symporter, which is mostly active during exponential growth phase during glucose consumption (Sá-Pessoa et al., 2013). In archaea, the *aceP* gene from *Methanosarcina acetivorans* was found to be overexpressed in the presence of acetate, however, this high level of expression is only reached when acetate is used as a sole carbon source (Rohlin and Gunsalus, 2010). The crystal structure of the SatP homolog from *Citrobacter koseri* (SatP_Ck) recently released, revealed a complex anion channel with four acetate-binding sites aligned in a single file interrupted by three hydrophobic constrictions (Qiu et al., 2018).

In this study, we carried out a deep phylogenetic analysis of AceTr family and functionally characterized new members of this family: the yeast GPR1 from *Y. lipolytica* and Fun34 from *S. cerevisiae* and the archaea aceP from *M. acetivorans*. Here we demonstrate the crucial role played by each residue of the conserved amino acid residues from the motif NPAPLGL(M/F). SatP molecular modelling studies allowed the identification of other amino acid residues essential for SatP activity.

2. Material and methods

2.1. Homology search

We downloaded over 10,000 proteomes from NCBI Assembly platform as individual FASTA files. A BLAST search, with a cut-off e-value 10^{-5}, was performed on this database using three queries, a bacterial, an archaeal and an eukaryotic member: Satp from the organism *E. coli*, AceP from *M. acetivorans* and Ady2 from *S. cerevisiae*. To avoid redundancies, only sequences from a single genome of a given species were considered.

2.2. Alignment and phylogenetic reconstruction

Retrieved protein sequences were aligned with PROMALS3D (Pei et al., 2008), a multiple-alignment algorithm that incorporates secondary structure prediction. Sequences that were not aligning extensively across the conserved region of the alignment were further excluded from the phylogenetic analysis. A phylogenetic reconstruction was performed using Maximum Likelihood, more appropriate for the deeper divergences under analysis here, using MEGA6 (Tamura et al., 2013) and the Jones-Taylor-Thornton (JTT) substitution model. Bootstrap was performed for 1000 repetitions. Obtained phylogenetic tree was displayed and edited in FigTree v.1.3.1 (http://tree.bio.ed.ac.uk/).

2.3. Three-dimensional modelling and molecular docking

The three-dimensional modelling analysis was performed for both SatP and Ady2, using as template the crystal structure of the SatP_Ck protein. The residue sequence of SatP and Ady2 were threaded in the Swiss-Model server (Bertoni et al., 2017) and the PDB file of SatP_Ck was added as a template model. Since SatP three-dimensional modelling obtained the best score for protein structure prediction, it was further considered for molecular docking analysis. Molecular docking simulations were performed as described before (Ribas et al., 2017).

2.4. Strains, plasmids and growth conditions

The strains and plasmids used in this work are listed in Tables 1 and 2 respectively. The *S. cerevisiae* strain W303-1A *jen*1Δ *ady*2Δ, lacking monocarboxylate uptake capacity, was used to express the *ADY2* alleles and the *GPR1* from *Y. lipolytica*. The cultures were maintained on slants of yeast extract (1%, w/v), peptone (1%, w/v), glucose (2%, w/v) and agar (2%, w/v) or yeast nitrogen base (Difco), 0.67%, w/v (YNB medium), supplemented with adequate requirements for prototrophic growth. For drop tests, cells were grown on YNB Glu-Ura media, until mid-exponential phase and diluted to an OD 640 nm of 0.1. A set of three 1:10 serial dilutions were performed and 3 µl of each suspension was inoculated in YNB acetic acid 0.5% (Oxoid agar 2%) pH 5.5, using YNB Glu-Ura as a control. Cells were incubated at 18 °C for 5 days. At 18 °C, carboxylic acid uptake by diffusion is drastically reduced, so that growth on carboxylic acid as sole carbon source is directly dependent on a functional transporter (Soares-Silva et al., 2007). The *E. coli* strain *actP*Δ *lldp*Δ *satP*Δ (assigned in this study as *E. coli* 3Δ) was used to express the *satP* alleles and the *aceP* gene from *M. acetivorans*. Bacterial strains were grown as previously described (Sá-Pessoa et al., 2013).

Table 1
List of plasmids used in this study.

Plasmid	Characteristics	Reference
pUC18	High-copy plasmid, constitutive expression	Norrander et al. (1983)
PSatP	pUC18 derivative; constitutive expression of *SatP*	Sá-Pessoa et al. (2013)
pSatP-N8A	pSatP with the substitution N8A in SatP	This study
pSatP-P9A	pSatP with the substitution P9A in SatP	This study
pSatP-A10T	pSatP with the substitution A10T in SatP	This study
pSatP-P11A	pSatP with the substitution P11A in SatP	This study
pSatP-L12A	pSatP with the substitution L12A in SatP	This study
pSatP-G13A	pSatP with the substitution G13A in SatP	This study
pSatP-L14A	pSatP with the substitution L14A in SatP	This study
pSatP-M15A	pSatP with the substitution M15A in SatP	This study
p416GPD	Glyceraldehyde-3-phosphate dehydrogenase (GPD) promoter	Mumberg et al. (1995)
pDS1::GFP	p416 derivative, constitutive expression of JEN1::GFP	Soares-Silva et al. (2007)
pAdy2::GFP	p416 derivative, constitutive expression of ADY2::GFP	This study
pAdy2::GFP-N89A	pAdy2::GFP with substitution N89A in Ady2	This study
pAdy2::GFP-P90A	pAdy2::GFP with substitution P90A in Ady2	This study
pAdy2::GFP-A91T	pAdy2::GFP with substitution A91T in Ady2	This study
pAdy2::GFP-P92A	pAdy2::GFP with substitution P92A in Ady2	This study
pAdy2::GFP-L93A	pAdy2::GFP with substitution L93A in Ady2	This study
pAdy2::GFP-G94A	pAdy2::GFP with substitution G94A in Ady2	This study
pAdy2::GFP-L95A	pAdy2::GFP with substitution L95A in Ady2	This study
pAdy2::GFP-S92A	pAdy2::GFP with substitution S92A in Ady2	This study
PAceP	pUC18 derivative; constitutive expression of *aceP*	This study
p416::Gpr1	p416GPD with constitutive expression of *GPR1*	This study
p416::Gpr1-GFP	p416GPD with constitutive expression of *GPR1::GFP*	This study

Table 2
List of strains used in this study.

Strain	Genotype	Reference
E. coli MG1693	thyA715	Arraiano et al. (1988)
E. coli Δ*lldP*	*MG1693 lldP (ΔlldP::Cm^R)*	This study
E. coli 3Δ	*MG1693 yaaH actP lldP (ΔyaaH /ΔactP/ΔlldP::Cm^R)*	This study
E. coli 3Δ pUC18	*E. coli* 3Δ transformed with pUC18	This study
E. coli 3Δ pSatP	*E. coli* 3Δ transformed with pSatP	This study
E. coli 3Δ pSatP-N8A	*E. coli* 3Δ transformed with pSatP-N8A	This study
E. coli 3Δ pSatP-P9A	*E. coli* 3Δ transformed with pSatP-P9A	This study
E. coli 3Δ pSatP-A10T	*E. coli* 3Δ transformed with pSatP-A10T	This study
E. coli 3Δ pSatP-P11A	*E. coli* 3Δ transformed with pSatP-P11A	This study
E. coli 3Δ pSatP-L12A	*E. coli* 3Δ transformed with pSatP-L12A	This study
E. coli 3Δ pSatP-G13A	*E. coli* 3Δ transformed with pSatP-G13A	This study
E. coli 3Δ pSatP-L14A	*E. coli* 3Δ transformed with pSatP-L14A	This study
E. coli 3Δ pSatP-M15A	*E. coli* 3Δ transformed with pSatP-M15A	This study
E. coli 3Δ pAceP	*E. coli* 3Δ transformed with pAceP	This study
S. cerevisiae W303-1A	MATα *ade2 leu2 his3 trp1 ura3*	Thomas and Rothstein (1989)
*S. cerevisiae jen*1Δ *ady*2Δ	W303-1A; *JEN1::KanMX4 ADY2::HphMX4*	Soares-Silva et al. (2007)
*S. cerevisiae jen*1Δ *ady*2Δ p416GPD	*jen*1Δ *ady*2Δ transformed with p416GPD	Soares-Silva et al. (2007)
*S. cerevisiae jen*1Δ *ady*2Δ pAdy2	*jen*1Δ *ady*2Δ transformed with *p416::Ady2*	This study
*S. cerevisiae jen*1Δ *ady*2Δ pAdy2::GFP	*jen*1Δ *ady*2Δ *transformed with pAdy2::GFP*	This study
*S. cerevisiae jen*1Δ *ady*2Δ pAdy2::GFP-N89A	*jen*1Δ *ady*2Δ *transformed with pAdy2::GFP-N89A*	This study
*S. cerevisiae jen*1Δ *ady*2Δ pAdy2::GFP-P90A	*jen*1Δ *ady*2Δ *transformed with pAdy2::GFP-P90A*	This study
*S. cerevisiae jen*1Δ *ady*2Δ pAdy2::GFP-A91T	*jen*1Δ *ady*2Δ transformed with pAdy2::GFP-A91T	This study
*S. cerevisiae jen*1Δ *ady*2Δ pAdy2::GFP-P92A	*jen*1Δ *ady*2Δ transformed with pAdy2::GFP-P92A	This study
*S. cerevisiae jen*1Δ *ady*2Δ pAdy2::GFP-L93A	*jen*1Δ *ady*2Δ transformed with pAdy2::GFP-L93A	This study
*S. cerevisiae jen*1Δ *ady*2Δ pAdy2::GFP-G94A	*jen*1Δ *ady*2Δ transformed with pAdy2::GFP-G94A	This study
*S. cerevisiae jen*1Δ *ady*2Δ pAdy2::GFP-L95A	*jen*1Δ *ady*2Δ transformed with pAdy2::GFP-L95A	This study
*S. cerevisiae jen*1Δ *ady*2Δ pAdy2::GFP-S92A	*jen*1Δ *ady*2Δ transformed with pAdy2::GFP-S92A	This study
Yarrowia lipolytica PYCC 4811	Wild-type	Collection
S. cerevisiae S288c	Wild-type	Collection
*S. cerevisiae jen*1Δ *ady*2Δ pGpr1	*jen*1Δ *ady*2Δ transformed with *p416::Gpr1*	This study
*S. cerevisiae jen*1Δ *ady*2Δ pGpr1-GFP	*jen*1Δ *ady*2Δ transformed with *p416::Gpr1-GFP*	This study

2.5. Construction of *E. coli actPΔ lldPΔ satPΔ*

The *lldP* null-mutant was constructed using the primer pairs dlldP1/dlldP2 and following the λ–red recombinase method (Datsenko and Wanner, 2000) with a few modifications, as described previously (Sá-Pessoa et al., 2013; Viegas et al., 2007). The chloramphenicol-resistance cassette of plasmid pKD3 replaces nucleotides +50 to +1587 of the *lldP* gene. The gene deletion was verified by colony PCR using the primer pair P1lldP/P2lldP and the chromosomal mutation subsequently transferred to a fresh genetic background (MG1693 strain) by P1 phage transduction, to generate *E. coli* MG1693 *lldP* (Δ*lldP*::Cm^R) strain. To construct the triple *yaaH/actP/lldP* mutant, the antibiotic resistance genes of the double *yaaH/actP* mutant (BBC234) (Sá-Pessoa et al., 2013) were eliminated using a helper plasmid encoding the FLP recombinase (pCP20) and following the procedures previously described (Datsenko and Wanner, 2000). The loss of the kanamycin and chloramphenicol resistance was confirmed, and the strain used as a receptor, in the P1 phage transduction of *lldP* mutation from the single *lldP* null-mutant. The chloramphenicol resistance was used for selection of the *lldP* mutation and the presence of the three, *yaaH*, *actP* and *lldP*, gene deletions were confirmed by PCR using specific primers: P1yaaH/P2yaaH for *yaaH*; P1ActP/P4actP for *actP* and P1lldP/P2lldP for *lldP* (primers listed in Supplementary Table S1).

Supplementary data associated with this article can be found, in the online version, at https://doi.org/10.1016/j.fgb.2018.10.001.

2.6. Cloning strategy of *aceP* gene

The *aceP* gene was chemically synthesized with an optimal codon usage for expression in *E. coli,* under the control of lac promoter. The synthetic *aceP* gene was codon optimized by the OptimumGene software tool (GenScript, Piscataway, NJ, USA Inc.). The synthetic version of *aceP* flanked by *Kpn*I and*Nde*I restriction sites was cloned in the puc18 vector, originating the pAceP vector.

2.7. Heterologous expression of *GPR1*

The pGPR1 plasmid was constructed by restriction enzyme cloning and the pGPR1::GFP plasmid through GAP repair technique (Bessa et al., 2012). The GPR1 gene was amplified by PCR, from genomic DNA extracted from *Yarrowia lipolytica* PYCC 4811 (Lõoke et al., 2011), using the primers Gpr1_FWD and Gpr1_REV (Supplementary Table S1). The amplified GPR1 was digested using *Hind*III and *Sal*I enzymes (*ThermoFisher Scientific*; USA). The final product was inserted into the vector p416GPD, previously digested with the same restriction enzymes using the same conditions. The resultant plasmid pGPR1 was cloned into *S. cerevisiae* W303-1A *jen*1Δ *ady*2Δ strain. To obtain the plasmid pGPR1-GFP, the GFP gene was inserted as described by Bessa et al. (2012), using the primers Gpr1-gfp_FWD and the Gpr1-gfp_REV (Supplementary Table S1).

2.8. Cloning strategy for *FUN34*

The pFUN34 plasmid was constructed by restriction enzyme cloning. The *FUN34* gene was amplified by PCR, from genomic DNA extracted from *S. cerevisiae S288c*, using the primers Fun34_FWD, Fun34_REV (Supplementary Table S1). The amplified versions were digested using *Bam*HI and *Xho*I enzymes considering. The final products were inserted into the vector p416GPD, previously digested with the same restriction enzymes using the same conditions. The final plasmid, pFUN34 was cloned into *S. cerevisiae* W303-1A *jen*1Δ *ady*2Δ strain.

2.9. Construction of Ady2 and SatP mutants

Site-directed mutagenesis was performed as previously described (Soares-Silva et al., 2007). For *GFP* fusion proteins with the *ADY2*, GAP repair technique was performed as previously described (Soares-Silva et al., 2007), using the primers listed in Supplementary Table S1.

2.10. Transport assays

Measurement of transport activity in yeast and bacterial strains was performed as previously described by Soares-Silva et al. (2007) and Sá-Pessoa et al. (2013), respectively. The radiolabeled substrates used were the following: [1-^{14}C] acetic acid, sodium salt (GE Healthcare, London, UK) and [2,3-^{14}C] succinic acid (Moravek Biochemicals, California, USA).

2.11. Epifluorescent microscopy

Microscopy analysis was performed as described in Soares-Silva et al. (2007) on a Leica DM5000B epifluorescent microscope with a Leica DFC 350FX R2 digital camera using the LAS AF V1.4.1 software.

3. Results

3.1. Phylogenetic analysis of AceTr family

A total of 818 hits were obtained for the BLAST search in the NCBI's Assembly database, using complete genomes only, with the 3 proteins of the AceTr family: Ady2, SatP, *and* AceP. Homologues were present across a wide range of organisms: most of them were detected in bacteria, archaea, and fungi. Hypothetical AceTr homologs were also detected in the genus *Leishmania,* three Viridiplantae and the Rhodophyta *Cyanidioschyzon merolae*. 12 sequences that lacked large conserved regions were excluded from a final dataset of 806 sequences. For a clear description of the tree, some sections were labelled as E1, E2, and P1 to P4. A detailed tree with all homolog nominations and bootstrap values is available in the Supplementary Fig. S1.

The Phylogenetic tree (Fig. 1) suggests a basal split between eukaryotic and prokaryotic organisms. Eukaryotes and prokaryotes form two monophyletic clades with an exception from each subclade. The exception in the eukaryotic clade is the protein of bacteria *Gordonia polyisoprenivorans*, which might be dubious, whereas the exception in prokaryotic clade is from the pathogenic trypanosome *Leishmania* genus, which likely represents a case of horizontal gene transfer. The prokaryotic subclade shows bacterial and archaeal homologs intertwined within the tree. The tree splits deeply into two branches, labelled P1-3 and P4 in Fig. 1. P4 contains mostly homologues present in the bacterial phylum Firmicutes, so far uncharacterized. P1-3 also contains another split between a clade containing a high percentage of

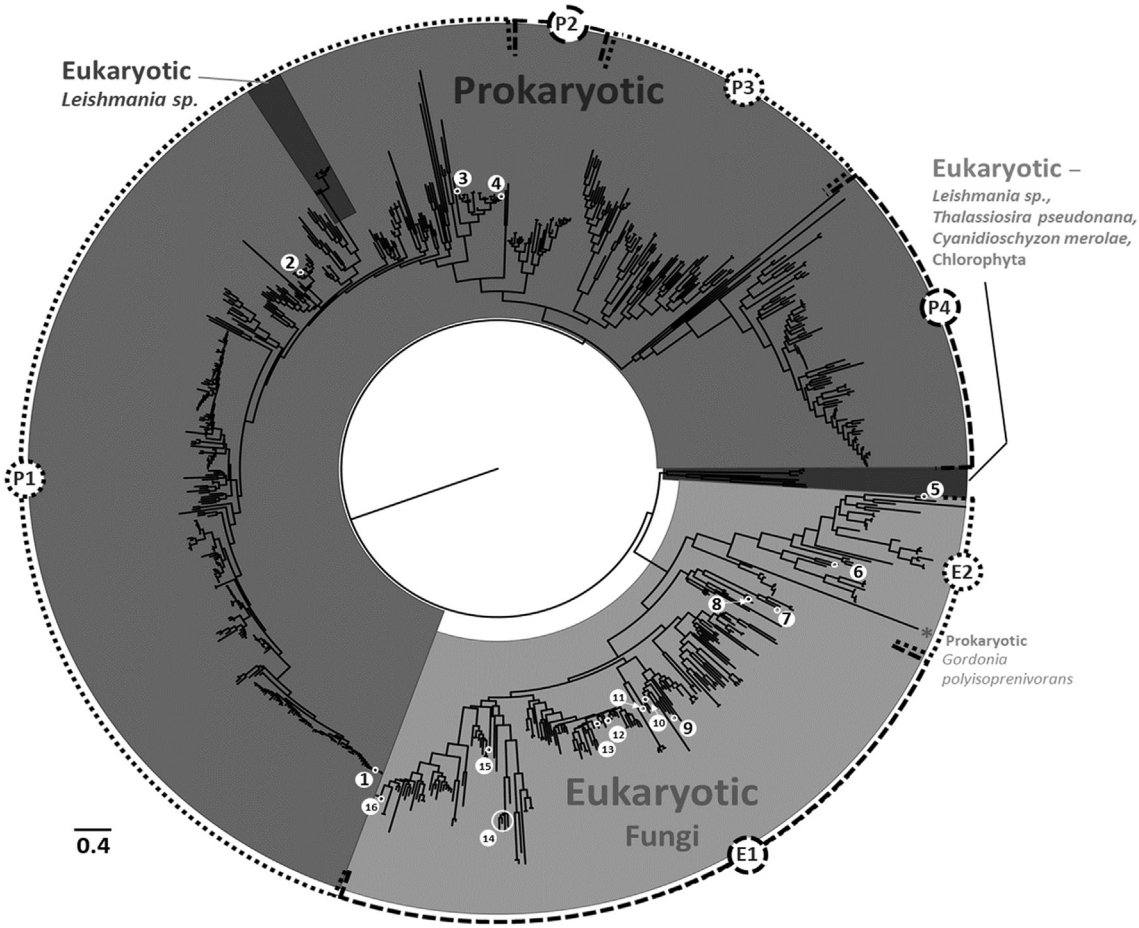

① *Escherichia Coli* (SATP)
② *Methanosarcina acetivorans* (MA_4008)
③ *Methanosarcina acetivorans* (MA_0103)
④ *Methanosarcina acetivorans* (MA_4393)
⑤ *Aspergilus nidulans* (AN8390)
⑥ *Aspergilus nidulans* (AN0366)
⑦ *Aspergilus nidulans* (acpC)
⑧ *Cryptococcus neoformans* (#1)
⑨ *Aspergilus nidulans* (*acpB*)
⑩ *Aspergilus nidulans* (acpA)
⑪ *Schizosaccharomyces pombe* (mug86)
⑫ *Saccharomyces cerevisiae* (ADY2)
⑬ *Saccharomyces cerevisiae* (ATO2)
⑭ *Yarrowia lipolytica* (#2)
⑮ *Yarrowia lipolytica* (GPR1)
⑯ *Saccharomyces cerevisiae* (ATO3)

#1 CNAG_05266,CNAG_05678,CNAG_04787,CNAG_05266
#2 YALI1_C32119g,YALI1_E15804g,YALI1_E32315g,YALI1_F17569g,YALI1_F21728g

Fig. 1. Maximum likelihood phylogenetic tree of AceTr family (TCDB 2.A.96) present in eukaryotic and prokaryotic genomes. Branch lengths are proportional to sequence divergence. Major taxonomic groups are indicated in different shades of grey. Homologues relevant for the discussion through the manuscript are highlighted. Groups indicated as E1, E2, P1, P2, P3, and P4 were created to facilitate the following of the tree description in the main text and are not meant to provide any type of classification.

homologues present in Actinobacteria (P3), a monophyletic archaea sub-branch and homologues from various other bacteria (including Phyla Firmicutes, Proteobacteria and others), and a second more frequent clade (P1-2) where bacterial homologues from phylum Proteobacteria are the most common (forming the totality of minor clade P2). The large subclade P1 also contains other bacteria, several archaea and the mentioned-above subclade of eukaryotic *Leishmania* genus. The P1 subclade contains the SatP from bacteria *E. coli* (Sá-Pessoa et al., 2013) and AceP (this study) from archaea *M. acetivorans*, two transporters functionally characterized as acetate transporters and two *M. acetivorans* homologues not functionally characterized (MA_0103 and MA_4393). It is important to note that while prokaryotic homologues dominate the tree, only 15% of the genomes in the database contained at least one member of the AceTr family (14% in bacteria and 31% in archaea), reflecting mostly the large numbers of sequenced prokaryotic genomes. The eukaryotic branch has a deep divergence between homologues present in fungi and other eukaryotes, *Leishmania* sp., *Thalassiosira pseudonana* (a marine diatom) abd *Cyanidioschyzon merolae* (red algae). The presence of this deep clade suggests a probable more ancient presence in a wider range of eukaryotes. Homologues belonging to the AceTr family were detected in 97% of the genomes analyzed in fungi. The large clade splits into two subclades. The minor (E2) holds mostly homologues present in filamentous ascomycetes. A second one (E1) includes homologues from a wider taxonomic range of fungi, including Basidiomycota and a few filamentous Ascomycetes, namely experimentally tested homologues in *Aspergillus nidulans AcpA, AcpB, and AcpC*. In the remaining clade, most sequences were mainly detected in Saccharomycetes, including a large sub-clade formed by Saccharomycetales only, although one subclade includes the AcpA and AcpB. The large clade containing only Saccharomycetales has the three homologues of *S. cerevisiae*. Ady2 and Fun34 are very similar phylogenetically with Ato3, suggesting a duplication and evolution of the gene dating to an earlier divergence within the Saccharomycetales evolution. This duplication probably occurred before the whole genome duplication event in yeast, since the yeasts *Kluyveromyces marxianus* and *Kluyveromyces lactis* have homologues in a cluster together with both Ady2/Fun34 and Ato3 from *S. cerevisiae*. This major clade of Saccharomycetales also holds the homologues of *Yarrowia lipolytica,* including the Gpr1 protein.

3.2. The aceP gene codes for an acetate permease

Methanosarcina acetivorans uses acetate as a source of carbon and as a source of energy by breaking down acetate to produce carbon dioxide and methane. It was previously shown that *aceP* gene from *M. acetivorans* is overexpressed in the presence of acetate (Rohlin and Gunsalus, 2010). The *M. acetivorans* species has an optimal growth temperature between 35 °C and 45 °C and optimal pH between 6.5 and 7.0 (Sowers et al., 1984), close to the model organism *E. coli,* which led us to attempt the heterologous expression of *aceP* in this last organism. In addition, the tools for genetic manipulation of *M. acetivorans* are scarce, and culture conditions are difficult to achieve. The heterologous expression of *aceP* was performed in the *E. coli* 3Δ strain, deleted for three monocarboxylate transporters, ActP an acetate transporter (Gimenez et al., 2003), LldP lactate transporter (Núñez et al., 2001), and SatP acetate/succinate (Sá-Pessoa et al., 2013). An optimized version of *aceP* was created using the GeneScript codon usage adaptation algorithm (GeneScript, USA). The vector pAceP was transformed in the *E. coli* 3Δ strain, and the acetate uptake measured after growth in minimal medium with glucose as a carbon source, during the exponential growth phase. The *E. coli* 3Δ pAceP was able to recover the mediated transport of acetate, with a Michaelis-Menten kinetics, displaying a K_m of 0.49 ± 0.07 mM of acetic acid and a V_{max} of 46.4 ± 2.9 nmol min^{-1} mg^{-1} protein (Fig. 2A).

The energetics of the acetate uptake in the *E. coli* 3Δ pAceP strain was further evaluated. We verified that the protonophore CCCP (carbonyl cyanide *m*-chlorophenylhydrazone), which collapses the proton motive force, lowered acetate transport to almost negligible values at pH 6.0 in cells expressing AceP (Fig. 2B). The potassium ionophore valinomycin and the sodium ionophore monensin, which disrupt the membrane electrical potential ($\Delta\psi$), had no significant effect on acetate uptake. These data suggest that acetate uptake occurs by a proton symporter mechanism, similar to other AceTr acetate transporter members yet functionally characterized: AcpA, AcpB, Ady2 and SatP. The measurement of labelled acetate uptake in the presence of non-labelled acids allowed the identification of potential inhibitors of acetic acid uptake, being indicative of an interaction of these acids with the transporter protein. None of the carboxylic acids tested inhibited the acetate uptake in *E. coli* 3Δ cells expressing *aceP* (Fig. 2C). Thus, this acetate transporter is not able to bind the carboxylic acids here tested, namely the monocarboxylates lactate, pyruvate and formate, and the dicarboxylates malate and succinate.

3.3. Gpr1 mediates acetate transport in S. cerevisiae

The functionality of the Gpr1 membrane protein from *Y. lipolytica* was accessed through heterologous expression in the *S. cerevisiae* W303-1A *jen*1Δ *ady*2Δ, a strain, which does not have activity for plasma

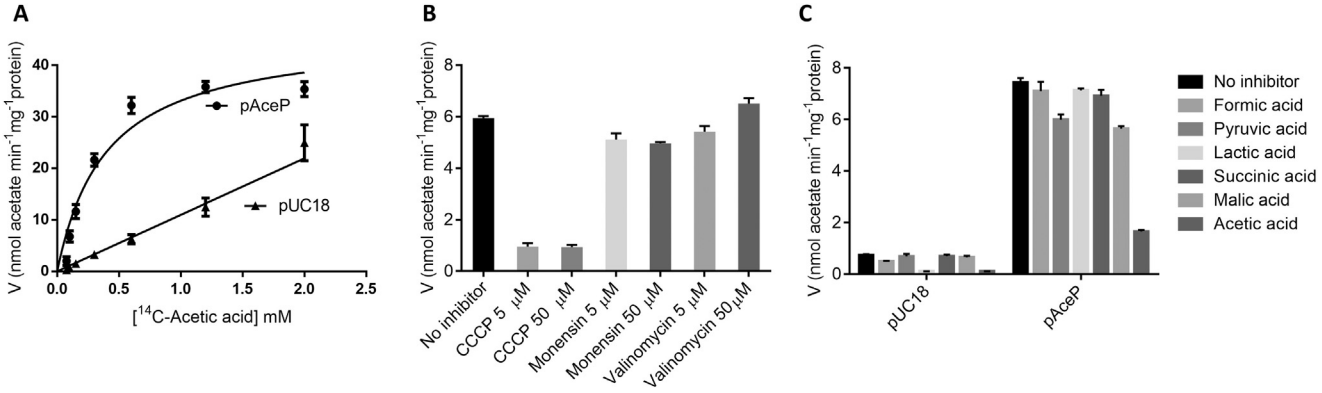

Fig. 2. Acetate uptake and transport energetics of *E. coli* 3Δ heterologously expressing pAceP: (A) Initial uptake rates of radiolabelled ^{14}C-acetic acid at different concentration by *E. coli* 3Δ heterologously expressing pAceP or pUC18, at pH 6.0, 30∘C; (b) Transport energetics: effect of CCCP, valinomycin, and monensin on the uptake of 0.1 mM ^{14}C-acetic acid in cells of *E. coli* 3Δ pAceP; C) transport specificity: the uptake of 0.1 mM ^{14}C-acetic acid in *E. coli* 3Δ heterologously expressing pAceP or pUC18 measured in the absence and presence of non-labelled formic, pyruvic, lactic, succinic and malic acid (10 mM), pH 6.0 and 30 °C. Cells were pre-incubated with the compounds mentioned, at the concentration indicated and pH 6.0 for 1 min before adding the radiolabelled substrate. Each data point represents the mean ± S.D. for three independent experiments (n = 9).

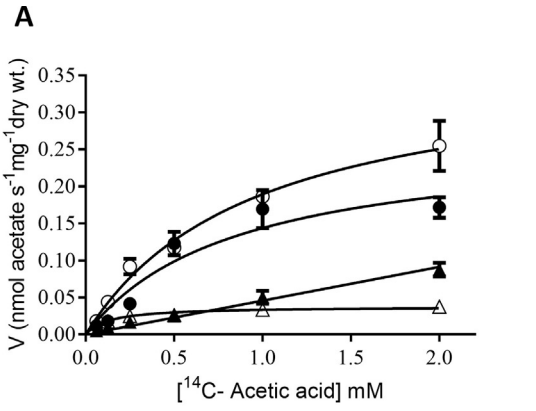

Plasmid	Km (mM)	Vmax (nmol acetate s^{-1} mg^{-1} dry wt.)
pAdy2	0.84 ± 0.26	0.27 ± 0.04
pGpr1	0.95 ± 0.21	0.37 ± 0.04

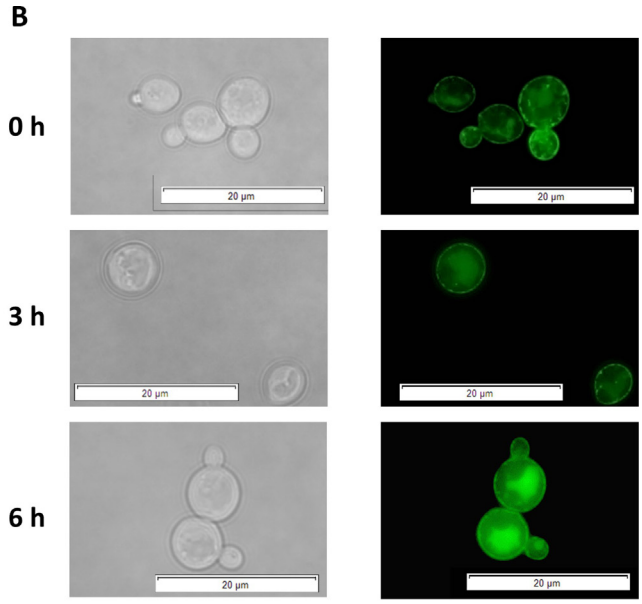

Fig. 3. (A) Initial uptake rates of radiolabeled ^{14}C-acetic acid at different concentrations by *S. cerevisiae* W303-1A *jen*1Δ *ady*2Δ cells heterologously expressing pGpr1, pAdy2, pFun34 and p416GPD as a control at pH 6.0, 30 °C and respective kinetic parameters. Cells were cultivated in glucose until exponential growth phase, washed and transferred to YNB supplemented with acetic acid (0.5%) during 6 h. Each data point represents the mean ± S.D. for three independent experiments (n = 9). (B) Epifluorescence and contrast phase microscopy of a GFP-tagged version of *S. cerevisiae* W303-1A *jen*1Δ *ady*2Δ cells expressing *GPR1*, before and during 6 h of exposure of cells to 0.5% acetic acid, at pH6, 30 °C. Scale bars = 20 µm.

membrane carboxylate mediated transport under the conditions tested (Queirós et al., 2007; Ribas et al., 2017; Soares-Silva et al., 2007; Soares-Silva et al., 2015). Mid-exponential *S. cerevisiae* cells expressing *GPR1* grown on glucose (minimal medium YNB-Glu) were collected, washed and incubated for 6 h in minimal medium containing 0.5% acetic acid (pH 6.0), as sole carbon and energy source. The expression of Gpr1 was able to restore the acetate-mediated transport in *S. cerevisiae jen*1Δ *ady*2Δ strain with a K_m of 1.13 ± 0.32 mM and V_{max} of 0.41 ± 0.06 nmol acetate s^{-1} mg^{-1} dry weight, at pH 6.0 (Fig. 3A). A GFP-tagged version of Gpr1p was analyzed by fluorescence microscopy revealing that the fusion protein was localized at the plasma membrane in glucose and acetic acid-grown cells for at least 6 h (Fig. 3B).

3.4. Fun34 does not transport acetate

Following the methodology described in the previous section, the activity of the Fun34 protein, the closest homologue of the acetate transporter Ady2 from *Saccharomyces cerevisiae*, was accessed by constitutive expression in the *S. cerevisiae jen*1Δ *ady*2Δ strain. The results revealed that the overexpression of Fun34 does not restore the mediated acetate transport at pH 6.0 (Fig. 3A).

3.5. The residues of the conserved motif NPAPLGL(M/S) are crucial for protein activity

The motif ^{89}NPAPLGL(M/S)^{96} (numbers refer to Ady2 sequence) exhibit an extensive conservation among the AceTr family members (Supplementary Fig. S2). Most of the conserved residues are polar and hydrophobic and thus have the potential to interact with charged substrates, e.g. acetate, succinate, a feature that was recently revealed by the 3D structure recently realized (Qiu et al., 2018). We performed site-directed mutagenesis both in the Ady2 and SatP conserved motif

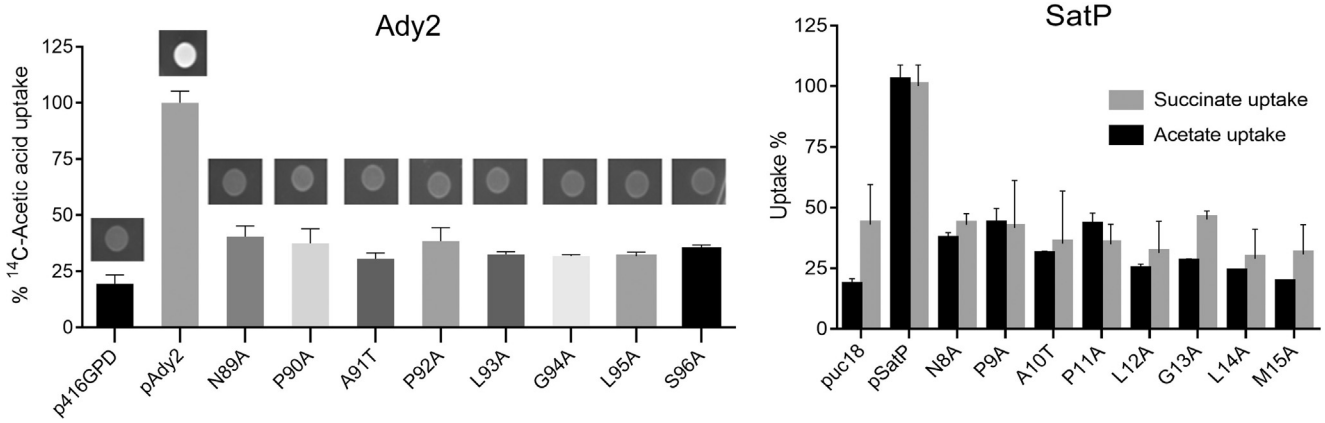

Fig. 4. (A) The percentage of 1 mM ^{14}C-acetic acid uptake, at pH 6.0, considering the velocity of transport found for the *S. cerevisiae ady*2Δ *jen*1Δ strains expressing pAdy2 as 100%. Cells were cultivated in glucose until mid-exponential growth phase, washed and transferred during 6 h to YNB supplement with the acetic acid (0.5%) and solid YNB acetic acid (0.5%) for growth tests shown in the images above each bar of Ady2 alleles and in p416GPD. B) The percentage of 0.5 mM ^{14}C-acetic acid uptake, at pH 6.0, considering the velocity of transport found for the *E. coli* 3Δ strains expressing pSatP as 100%. Cells were collected at mid-exponential growth phase from minimal medium with glucose 1% (w/v). Each data point represents the mean ± S.D. for three independent experiments (n = 9).

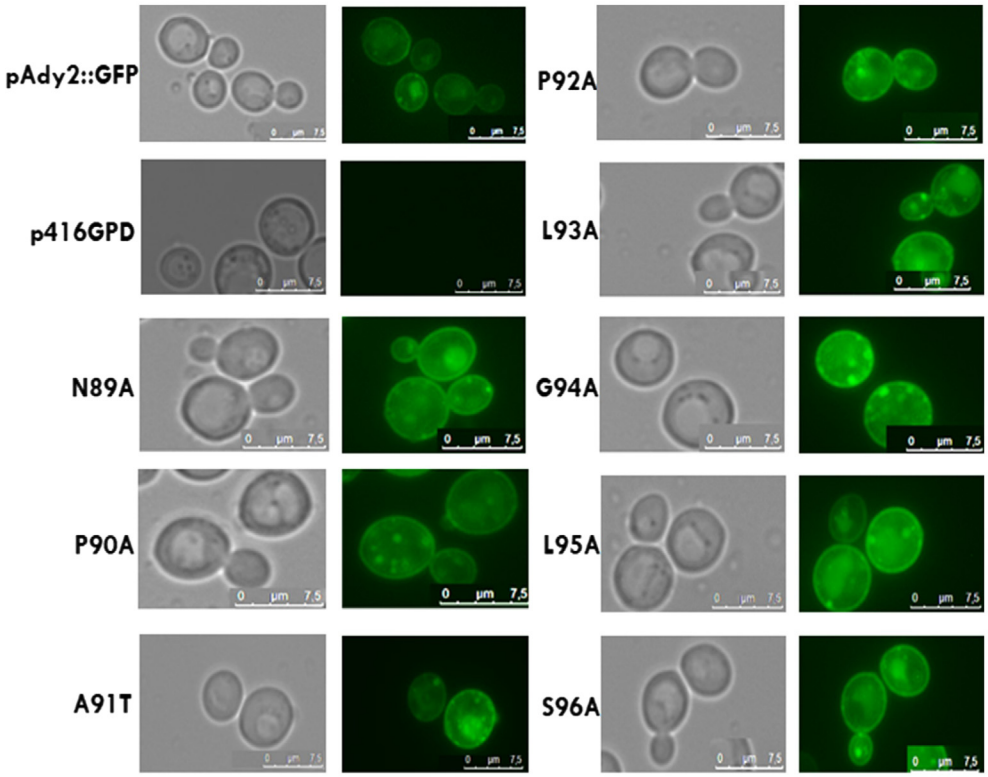

Fig. 5. Epifluorescence microscopy localization of Ady2::GFP and mutant alleles expressed in *S. cerevisiae ady2Δ jen1Δ*. Cells were collected at mid-exponential growth phase from YNB glucose 1% (w/v), washed and transferred during 6 h to YNB, supplement with the acetic acid (0.5%), and observed by epifluorescence microscopy.

NPAPLGL(M/S) by replacing each residue by an alanine residue, except for the alanine residues 91 (Ady2) and 10 (SatP), which were both replaced by tyrosine residues. All the single mutations, from both Ady2 or SatP, decreased acetate transport (Fig. 4 A, B). Accordingly, all Ady2 mutant alleles displayed poor growth in YNB acetic acid (0.5%) as sole carbon and energy source when compared with the native allele. Since SatP is known to mediate the transport of succinate, we also measured succinate uptake in the SatP mutant alleles (Fig. 4B). Similar to acetate uptake, the SatP mutant alleles displayed a succinate uptake capacity significantly reduced when compared to the wild-type allele. In order to distinguish whether this is due to an incorrect protein location or lack of transporter function, we used mutant alleles expressing an Ady2::GFP chimeric transporter. In all Ady2 mutants, proteins were localized by epifluorescence microscopy at the plasma membrane (Fig. 5). These results strongly suggest that in these mutants presenting low or no transport capacity, the lack of transporter activity is not a consequence of altered protein trafficking, but rather due to a modification on the mechanism of substrate transport *per se*.

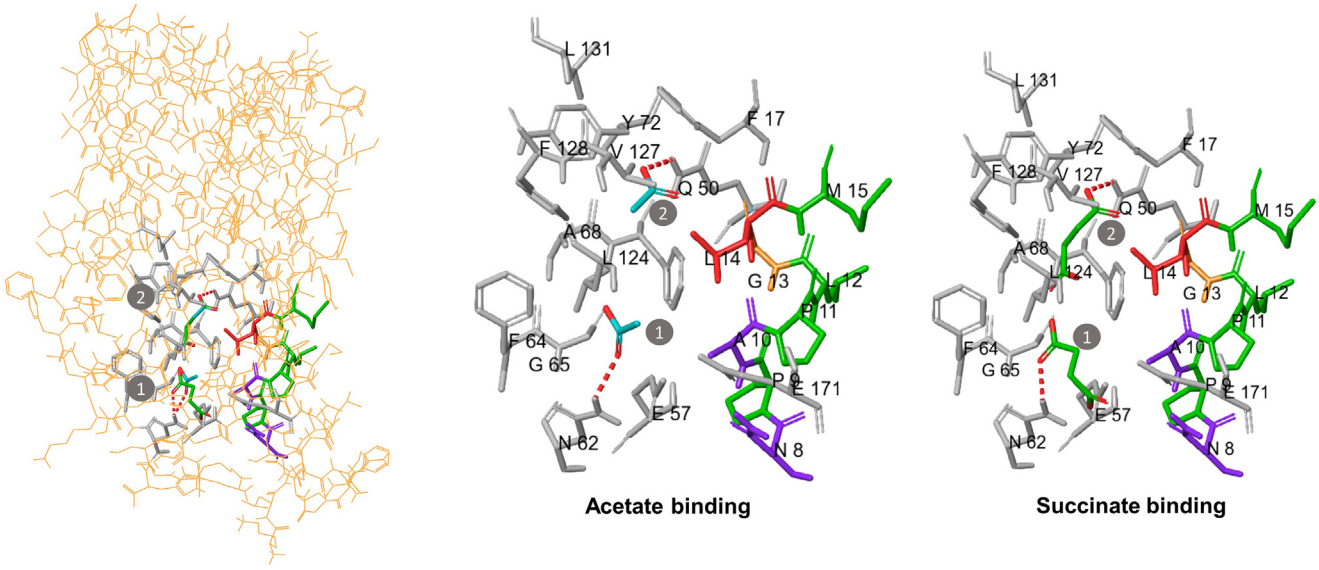

Fig. 6. Molecular docking of SatP 3D model, based on SatP_Ck structure, with the substrates acetate and succinate. Transversal (A) and cytoplasmic (B) view of SatP 3D model with the identification of the NPAPLGLM motif colored in black side chains. (C) Zoomed transversal view of the binding sites S1 and S2 for acetate and succinate, with the putative binding residues of the NPAPLGL motif colored in red side chains (N8, A10, G13, L14). (For interpretation of the references to colour in this figure legend, the reader is referred to the web version of this article.)

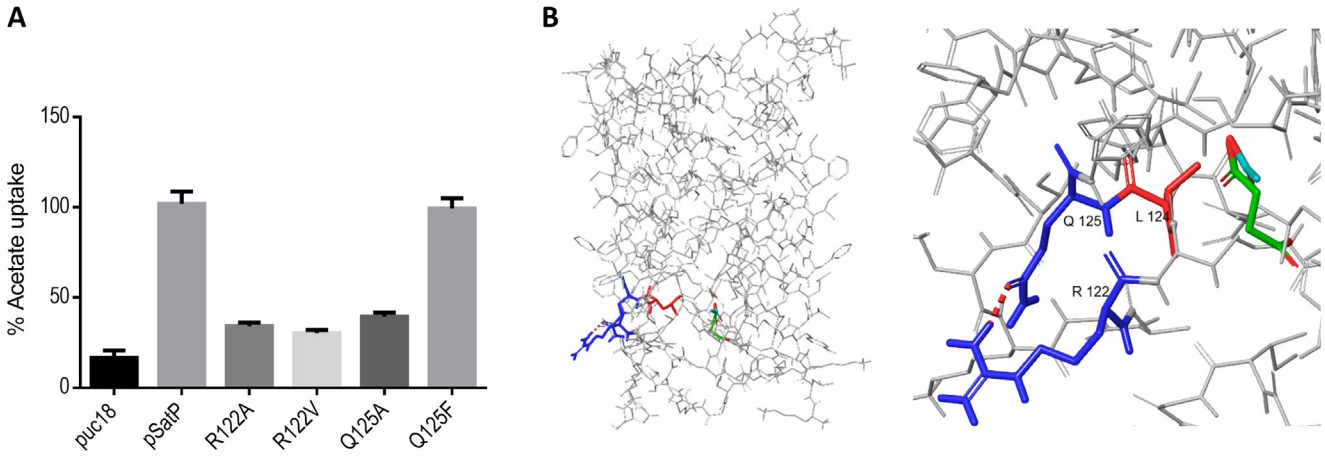

Fig. 7. (A) Transversal and cytoplasmic view of SatP 3D model obtained with the identification of the R122 and Q125 in blue side chains and the identification of the NPAPLGM residues in black side chains. Dash red line is indicative of hydrogen bonds. (B) The percentage of 0.5 mM ^{14}C-acetic acid uptake, at pH 6.0, considering the velocity of transport found for the *E. coli* 3Δ strains expressing pSatP as 100%. Cells were collected at mid-exponential growth phase from minimal medium with glucose 1% (w/v). Each data point represents the mean ± S.D. for three independent experiments (n = 9). (B). (For interpretation of the references to colour in this figure legend, the reader is referred to the web version of this article.)

3.6. SatP 3D model

Molecular docking based on a SatP 3D model obtained from the crystal structure of SatP_Ck (PDB 5YS3) uncovered the residues involved in acetate and succinate binding of the conserved motif NPAPLGLM (Fig. 6A, B), located in TMS 1. The residues N8, A10, G13, were identified as putative binding residues in the binding site S1, whereas the residues G13, L14, were identified as putative binding residues in the binding site S2. The SatP model suggests that succinate uses that same binding sites (S1 and S2) as acetate (Fig. 6C).

The SatP 3D model was used to identify novel residues essential for transporter's activity. A predicted hydrogen bond was found between the residues R122 and Q125 are facing the cytoplasmic side, at the beginning of the TMS 5 (Fig. 7A). The replacement of the R122 by an alanine or a valine (the Ady2 equivalent residue) reduced significantly the acetate uptake (Fig. 7B). The replacement of the Q125 by an alanine resulted in the abolishment, while the replacement by phenylalanine (the Ady2 equivalent residue) had no impact on acetate uptake (Fig. 7B).

4. Discussion

The AceTr-Acetate Transporters are found in all domains of life. The phylogenetic analysis of all the homologues so far sequenced, suggests a basal split between eukaryotic and prokaryotic organisms that form two monophyletic clades. Overall, the phylogenetic tree indicates that an ancestral form of this family was present in the primordial organisms in the root of the tree of life. However, although present in a taxonomically diverse range of organisms, the AceTr homologues are limited to very specific groups of prokaryotic and eukaryotic organisms. This fact strongly appoints to their loss in most organisms during evolution. While this trend is obvious for most eukaryotic organisms outside fungi (homologues detected in only 10% of analyzed genomes), the picture is similar for prokaryotic organisms, with members of the AceTr family detected in only 15% of the genomes in the database. On a drastic shift, homologues were detected in 97% of the fungal genomes analyzed. These data suggest that these transporters play a key role in fungi. In fact, the Ady2 from *S. cerevisiae* was described as essential for proper ascus formation (Rabitsch et al., 2001) and later AcpA from *A. nidulans* as the major acetate transporter during germination of conidiospores (Sá-Pessoa et al., 2015). In addition, the Ady2 homologue of *Cryptococcus neoformans* was also associated with acetate transport and described as indispensable for survival during physiologically relevant starvation conditions (Kisirkoi, 2017). According to the phylogenetic analysis, the only fungal genomes without AceTr members were the *Encephalitozoon,* atypical fungi that belong to phylum Microsporidia (Katinka et al., 2001). Based on this evidence, it is tempting to postulate that this family of transporters is critical for spore germination process in fungi, and thus greatly conserved throughout evolution.

In this work, we extended the number of AceTr members functionally characterized as acetate transporters, and for the first time to an archaea member, the *aceP* gene from *M. acetivorans*. The *Methanosarcineae* are the most metabolically diverse methanogens, that thrive in a broad range of environments, and are unique among the Archaea in forming complex multicellular structures. Species, like *M. acetivorans* display high methanogenesis metabolic activity. In nature, the methane produced is mostly derived from acetate with a strong impact on global warming (Galagan et al., 2002). Here we demonstrate that the *aceP* from *M. acetivorans* is highly specific for acetate. Additionally, we characterized the acetate transport capacity of Gpr1 from *Y. lipolytica*, an AceTr family member, until now only described as being involved in cells sensitivity to acetic acid (Augstein et al., 2003). Gpr1p was reported to have an important role over stress cue, triggered by the exposure of cells to acetic acid, and to be involved in the repression of genes that encode glyoxylate cycle enzymes (Augstein et al., 2003; Tzschoppe et al., 1999). Fluorescence microscopy analysis of *S. cerevisiae* cells harbouring Gpr1-GFP revealed that the fusion protein was detected at the plasma membrane, as previously reported (Augstein et al., 2003; Matthäus and Barth, 2013). The yeast *Y. lipolytica* displays specific physiological, metabolic and genomic characteristics, which differentiates it from the model yeast *S. cerevisiae* (Nicaud, 2012). Although the whole genome duplication event did not occur in *Y. lipolytica*, its genome size is almost the double of *S. cerevisiae* having six AceTr members. Nevertheless, Gpr1 and Ady2, two of the AceTr members of these phylogenetically distant yeast species, maintained their activity as acetate transporters over evolution. We also found that the closest homologue of Ady2 in *S. cerevisiae*, the Fun34 membrane protein (sharing 70% amino acid identity with Ady2), is not involved in acetate transport. The differences found in acetate uptake between the strain expressing the empty vector and the strain overexpressing a nonfunctional protein (Fun34) is, most probably, related with the alteration of membrane composition that affects the diffusion of the acid across the plasma membrane.

To gain insights into the structure of AceTr family members, the conserved motif NPAPLGL(M/S) of Ady2 and SatP proteins, was analyzed by site-directed mutagenesis. The substrate uptake in these two

proteins was significantly reduced when each of the residues of the domain was mutated. However, these same mutant alleles did not affect plasma membrane targeting of Ady2. Accordingly the recently released SatP_Ck 3D structure, an ortholog of SatP, the conserved motif NPAPLGL(M/S) is located at the cytoplasmic vestibule of the protein, in the vicinity of the first (S1) and second (S2) acetate binding sites (Qiu et al., 2018). Our molecular docking analysis using SatP 3D model uncovered two putative binding sites accepting both acetate and succinate as substrates. Is it also noticeable that the residues N8, A10, L13 e G14 are the residues involved in the S1 and S2 binding sites, as it is highlighted in Fig. 6 in red side chains. The N8 residue was previously described as essential for protein activity since the N8A mutant allele lost almost all acetate conductivity (Qiu et al., 2018). The F17 and L14 residues were reported as essential players in the S2 binding site, determining the flux direction of the acetate anions and creating hydrophobic constriction sites (Qiu et al., 2018). Our results demonstrate the impact of the NPAPLGL(M/S) conserved residues in acetate uptake and reinforce their role as S1 and S2 binding sites (Qiu et al., 2018). Here, we also describe the role of SatP R122 and Q125 residues in substrate acetate uptake. According to the SatP 3D model, the charged R122 and polar Q125 form a hydrogen bond (see arrow, Fig. 7A) and are located in the cytoplasmic side, in the opposite position of the S1 binding site. Most probably these residues may help to attract negatively charged acetate/succinate anions to the cytoplasmic vestibule through electrostatic interactions as proposed by Qiu and colleagues (2018). The proposed structure for the SatP_CK protein discloses a hexamer structure, acting as a channel (Qiu et al., 2018). The monomers of the hexamer are reported to function independently and to transport different anions, such as acetate. The substrate transport is dependent on four binding sites for acetate and regulated by a gated mechanism in the interior of the pore of each monomer. The SatP_CK homologues Ady2, SatP, AceP and Gpr1 have been experimentally demonstrated to function as proton symporters, with the acetate uptake fitting to a Michaelis-Menten kinetics. In addition, proton flux studies (Ady2) and transport energetic assays (SatP, AceP) support their assignment as permeases dependent on proton-motif force (Casal et al., 1996; Paiva et al., 2004; Sá-Pessoa et al., 2013). Both the conclusion based on our data and that of Qiu et al. (2018) are well supported. Although both studies seem contradictory the differences might arise from differences in experimental methodologies. We think that to fully determine - whether members of the AceTr family act as channels or permeates further studies are required.

Acetate is a ubiquitous compound used by cells in distinct metabolic pathways (Xiao and Wu, 2014). In this work, we demonstrated that the AceTr family is widespread in bacteria, archaea, fungi and nematodes, with a prevalence close to 100% in fungi organisms. Acetate transporters of this family have been reported to play a role in normal sporulation of fungi organisms, development of asci (dyads) (Rabitsch et al., 2001), survival during physiologically relevant starvation conditions (Kisirkoi, 2017), cell and colony morphology, yeast-to-hyphae transition and cell lifespan (Augstein et al., 2003; Tzschoppe et al., 1999), which explains the wide distribution of AceTr family in the tree of life and specially the elevated prevalence found in fungi organisms. In addition, we disclosed the role of eleven amino acid residues in the substrate transport activity of AceTr transporters, namely the residues of the conserved motif NPAPLGL(M/S), which we propose to be considered the signature motif of AceTr family.

Acknowledgements

This work was supported by the strategic program UID/BIA/04050/2013 (POCI-01-0145-FEDER-007569) and the project PTDC/BIAMIC/5184/2014 funded by national funds through the Fundação para a Ciência e Tecnologia (FCT) I.P. and by the European Regional Development Fund (ERDF) through the COMPETE 2020 - Programa Operacional Competitividade e Internacionalização (POCI); by the project EcoAgriFood: Innovative green products and processes to promote AgriFood BioEconomy (operação NORTE-01-0145-FEDER-000009), supported by Norte Portugal Regional Operational Programme (NORTE 2020), under the PORTUGAL 2020 Partnership Agreement, through the European Regional Development Fund (ERDF). Work at ITQB NOVA was financially supported by Project LISBOA-01-0145-FEDER-007660 (Microbiologia Molecular, Estrutural e Celular) funded by FEDER funds through COMPETE2020 - Programa Operacional Competitividade e Internacionalização (POCI). DR acknowledges FCT for the SFRH/BD/96166/2013 PhD grant. MSS acknowledges the Norte2020 for the UMINHO/BD/25/2016 PhD grant with the reference NORTE-08-5369-FSE-000060.

We dedicated the article to the memory of Professor André Goffeau.

Conflict of interest

None declared.

References

Arraiano, C.M., Yancey, S.D., Kushner, S.R., 1988. Stabilization of discrete mRNA breakdown products in ams pnp rnb multiple mutants of Escherichia coli K-12. J. Bacteriol. 170 (10), 4625–4633.
Augstein, A., et al., 2003. Characterization, localization and functional analysis of Gpr1p, a protein affecting sensitivity to acetic acid in the yeast *Yarrowia lipolytica*. Microbiology 149, 589–600.
Bertoni, M., et al., 2017. Modeling protein quaternary structure of homo- and hetero-oligomers beyond binary interactions by homology. Sci. Rep. 7, 10480.
Bessa, D., et al., 2012. Improved gap repair cloning in yeast: treatment of the gapped vector with Taq DNA polymerase avoids vector self-ligation. Yeast 29, 419–423.
Casal, M., et al., 1996. Mechanisms regulating the transport of acetic acid in *Saccharomyces cerevisiae*. Microbiology 142 (Pt 6), 1385–1390.
Casal, M., et al., 2008. Transport of carboxylic acids in yeasts. FEMS Microbiol. Rev. 32, 974–994.
Casal, M., et al., 2016. Carboxylic Acids Plasma Membrane Transporters in *Saccharomyces cerevisiae*. Adv. Exp. Med. Biol. 229–251.
Datsenko, K.A., Wanner, B.L., 2000. One-step inactivation of chromosomal genes in *Escherichia coli* K-12 using PCR products. PNAS 97, 6640–6645.
Fillinger, S., Felenbok, B., 1996. A newly identified gene cluster in *Aspergillus nidulans* comprises five novel genes localized in the alc region that are controlled both by the specific transactivator AlcR and the general carbon-catabolite repressor CreA. Mol. Microbiol. 20, 475–488.
Flipphi, M., et al., 2006. Functional analysis of alcS, a gene of the alc cluster in *Aspergillus nidulans*. Fungal Genet. Biol. 43, 247–260.
Galagan, J.E., et al., 2002. The genome of *M. acetivorans* reveals extensive metabolic and physiological diversity. Genome Res. 12, 532–542.
Gimenez, R., et al., 2003. The gene *yjcG*, cotranscribed with the gene acs, encodes an acetate permease in *Escherichia coli*. J. Bacteriol. 185, 6448–6455.
Katinka, M.D., et al., 2001. Genome sequence and gene compaction of the eukaryote parasite *Encephalitozoon cuniculi*. Nature 414, 450.
Kisirkoi, G., 2017. Acetate transport is essential for survival and virulence of *Cryptococcus neoformans*. All Dissertations 1915.
Lõoke, M., et al., 2011. Extraction of genomic DNA from yeasts for PCR-based applications. Biotechniques 50, 325–328.
Matthäus, F., Barth, G., 2013. The Gpr1/Fun34/YaaH Protein Family in the Nonconventional Yeast *Yarrowia lipolytica* and the Conventional Yeast *Saccharomyces cerevisiae*. In: Barth, G. (Ed.), Yarrowia lipolytica: Genetics, Genomics, and Physiology. Springer Berlin Heidelberg, Berlin, Heidelberg, pp. 145–163.
Mumberg, D., Müller, R., Funk, M., 1995. Yeast vectors for the controlled expression of heterologous proteins in different genetic backgrounds. Gene 156 (1), 119–122.
Nicaud, J.-M., 2012. Yarrowia lipolytica. Yeast 29, 409–418.
Norrander, J., et al., 1983. Construction of improved M13 vectors using oligodeoxynucleotide-directed mutagenesis. Gene 26, 101–106.
Núñez, M.F., et al., 2001. The gene yghK linked to the glc operon of Escherichia coli encodes a permease for glycolate that is structurally and functionally similar to L-lactate permease. Microbiology 147, 1069–1077.
Paiva, S., et al., 2004. Ady2p is essential for the acetate permease activity in the yeast *Saccharomyces cerevisiae*. Yeast 21, 201–210.
Palková, Z., et al., 2002. Ammonia pulses and metabolic oscillations guide yeast colony development. Mol. Biol. Cell. 13, 3901–3914.
Pei, J., et al., 2008. PROMALS3D: a tool for multiple protein sequence and structure alignments. Nucl. Acids Res. 36, 2295–2300.
Qiu, B., et al., 2018. Succinate-acetate permease from *Citrobacter koseri* is an anion channel that unidirectionally translocates acetate. Cell Res.
Queirós, O., et al., 2007. Functional analysis of *Kluyveromyces lactis* carboxylic acids permeases: heterologous expression of *KlJEN1* and *KlJEN2* genes. Curr. Genet. 51, 161–169.
Rabitsch, K.P., et al., 2001. A screen for genes required for meiosis and spore formation based on whole-genome expression. Curr. Biol. 11, 1001–1009.
Ribas, D., et al., 2017. Yeast as a tool to express sugar acid transporters with

biotechnological interest. FEMS Yeast Res. 17.
Robellet, X., et al., 2008. AcpA, a member of the GPR1/FUN34/YaaH membrane protein family, is essential for acetate permease activity in the hyphal fungus *Aspergillus nidulans*. Biochem. J. 412, 485–493.
Rohlin, L., Gunsalus, R.P., 2010. Carbon-dependent control of electron transfer and central carbon pathway genes for methane biosynthesis in the Archaean, *Methanosarcina acetivorans* strain C2A. BMC Microbiol. 10, 62.
Sá-Pessoa, J., et al., 2015. Expression and specificity profile of the major acetate transporter AcpA in *Aspergillus nidulans*. Fungal Genet. Biol. 76, 93–103.
Sá-Pessoa, J., et al., 2013. SATP (YaaH), a succinate-acetate transporter protein in *Escherichia coli*. Biochem. J. 454, 585–595.
Soares-Silva, I., et al., 2007. The conserved sequence NXX[S/T]HX[S/T]QDXXXT of the lactate/pyruvate:H(+) symporter subfamily defines the function of the substrate translocation pathway. Mol. Membr. Biol. 24, 464–474.
Soares-Silva, I., et al., 2015. The *Debaryomyces hansenii* carboxylate transporters Jen1 homologues are functional in *Saccharomyces cerevisiae*. FEMS Yeast Res. 15, fov094.
Sowers, K.R., et al., 1984. Methanosarcina acetivorans sp. nov., an acetotrophic methane-producing bacterium isolated from marine sediments. Appl. Environ. Microbiol. 47, 971–978.
Tamura, K., et al., 2013. MEGA6: molecular evolutionary genetics analysis Version 6.0. Mol. Biol. Evol. 30, 2725–2729.
Thomas, B.J., Rothstein, R., 1989. Elevated recombination rates in transcriptionally active DNA. Cell 56 (4), 619–630.
Tzschoppe, K., et al., 1999. trans-dominant mutations in the *GPR1* gene cause high sensitivity to acetic acid and ethanol in the yeast *Yarrowia lipolytica*. Yeast 15, 1645–1656.
Viegas, S.C., et al., 2007. Characterization of the role of ribonucleases in Salmonella small RNA decay. Nucl. Acids Res. 35, 7651–7664.
Xiao, M., Wu, F., 2014. A review of environmental characteristics and effects of low-molecular weight organic acids in the surface ecosystem. J. Environ. Sci. 26, 935–954.